JAES | JOURNAL OF APPLIED ENGINEERING SCIENCE | www.engineeringscience.rs
ISTRAŽIVANJA I PROJEKTOVANJA ZA PRIVREDU

Indexed by

INVERSE DISTANCE INTERPOLATION FOR USED IN UNSTRUCTURED MESH FINITE VOLUME SOLVER

Adek Tasri
Mechanical Engineering Department,
Universitas Andalas, Padang 25163,
Indonesia

Key words: *inverse distance interpolation, finite volume, unstructured mesh*
doi:10.5937/jaes0-34022

Cite article:

Tasri A. (2022) SLIDING WEAR CHARACTERISTICS OF BORON CARBIDE AND NOVEL SQUID QUILL ASH INVERSE DISTANCE INTERPOLATION FOR USED IN UNSTRUCTURED MESH FINITE VOLUME SOLVER, *Journal of Applied Engineering Science*, 20(2), 597 - 601, DOI:10.5937/jaes0-34022

Online aceess *of full paper is available at: www.engineeringscience.rs/browse-issues*

Original Scientific Paper

Istraživanja i projektovanja za privredu
Journal of Applied Engineering Science

doi:10.5937/jaes0-34022 Paper number: 20(2022)2, 966, 597-601

INVERSE DISTANCE INTERPOLATION FOR USED IN UNSTRUCTURED MESH FINITE VOLUME SOLVER

Adek Tasri*

Mechanical Engineering Department, Universitas Andalas, Padang 25163, Indonesia

This article discusses adjusting inverse distance interpolation for use in unstructured mesh finite volume solutions. The adjustment was made on the weight function of the inverse distance interpolation using the Laplacian of the flow variable inside a Voronoi-dual of finite volume cells. We tested the accuracy of the adjusted inverse distance interpolation on two-dimensional potential flows. It was found that the adjusted and standard inverse distance interpolations have a similar degree of accuracy when used in unstructured, Delaunay based, finite volume mesh. However, the L1 norm error of the adjusted version of the inverse distance interpolation was much smaller than the L1 norm error of the standard version.

Key words: inverse distance interpolation, finite volume, unstructured mesh

INTRODUCTION

Interpolation methods are one of the key issues for accurate and efficient implementation of the finite volume method [1,2]. Interpolation from cell centres to vertices is routinely done to aid the field plotting of variables. However, it is also used by some flow computation algorithms, for example, to facilitate the integration of variables around cell boundaries for evaluation of derivatives from Gauss' theorem. One of the most common interpolations in finite volume is Inverse Distance Weighted (IDW) interpolation. The scheme was firstly suggested by Sheppard [3] for used as an interpolation scheme of discrete data. This method was then adopted to the finite volume method by Frink [4], even by the most popular commercial CFD, Fluent [5]. IDW was also used in a solution-adaptive scheme for solving partial differential equations by Shen [6]. Akima [7] used IDW interpolation for a surface fitting irregularly distributed data point. However, IDW interpolation was found to be inaccurate, especially when the sample points are distributed in the form of clusters [8, 9]. Gotway et al. [10] report bull-eye pattern error in contour plot of data interpolated using IDW. Several methods to improve Shepard's interpolation have been proposed in the literature in the past several years. Hooyberghs et al. [11] and Golkhatmi et al. [12] used a gradient of interpolation data to improve the accuracy of inverse distance interpolation. Ke et al. [13] used adaptive inverse distance weight based on clustering sample points. Franke and Nielson [14] and Ohtake et al. [15] proposed improving accuracy by using data from nearby points. Liu et al. [16] improve the accuracy of inverse distance interpolation used in three-dimensional geological modelling. The improvement was made by using spatial differentiation of geological attribute data. Modification of inverse distance interpolation for use in finite volume solutions reported by Henderson and Pena [17]. They developed a simplified version of inverse distance interpolation for finite volume solution of the advection flow. So far, the improvements have not been adequate for use in finite volume schemes because it based on scattered data assumptions, which is not entirely suitable for finite volume cases that deal with distributed data. In this study, We improve the accuracy of IDW interpolation used in finite volume solution of transport equation by adjusting the weight function of the interpolation based on the Laplacian of the flow variable inside a Voronoi-dual of the finite volume cells. The adjusted interpolation scheme was tested on a two-dimensional potential flow around an isolated cylinder in a uniform stream and the flow around Joukowsky aerofoil.

INVERSE DISTANCE WEIGHTED INTERPOLATION

Inverse distance interpolation is basically global in that they use all data points in the domain to calculate each interpolation value. These schemes assume that the interpolated value should be influenced more by near points and less by the more distant points. The interpolation value at each interpolation point is a weighted average of the values at the scattered surrounding points. The weight assigned to each scatter point diminishes as the distance from the interpolation point increases. The IDW interpolation formula for interpolation of variable at vertex v from surrounding cell centre i in finite volume mesh, as shown in Fig. 1, may be written as:

$$\varphi_v = \frac{\sum_{i=1}^{m} \frac{1}{l_i^k} \varphi_i}{\sum_{i=1}^{m} \frac{1}{l_i^k}} \quad (1)$$

m represent the number of cell centre surrounding the vertex v. l_i is the Euclidean distance between cell centre i and vertex v

*adek.tasri@eng.unand.ac.id

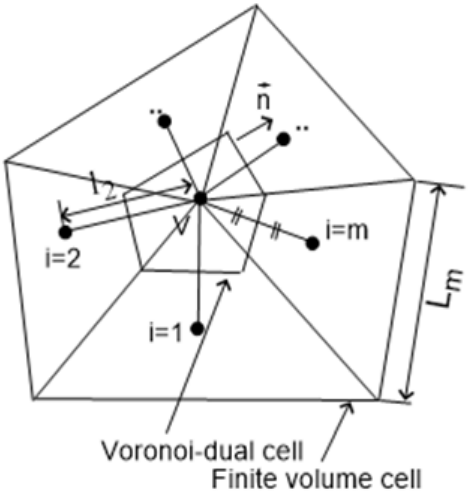

Figure 1: Control volume and Voronoi-dual cell around a cell vertex

Eq. (1) shows that as vertex v approaches cell i , φ_v tends to the value of φ_i and φv will be bounded above by max φ_i and below by min φ_i. Shepard [3] determined the exponent k in Eq. (1) from consideration of the differentiability of the interpolated field with respect to x and y axis. No derivatives exist for k < 1, whilst values of k > 2 tended to make the interpolated surface relatively flat around data points. Empirically then, Shepard chose k=2. Some studies to select the value of k resulted in the conclusion that the value of k = 2 is the best for most cases [18]. Frink [4] used this type of interpolation with an unstructured mesh code for calculation of potential flow around an aerofoil where only data at cell centre points immediately surrounding a vertex were used in the procedure. Frink [4] found that k=1 gives the most accurate result.

IMPROVED INVERSE DISTANCE INTERPOLATION

Because the inverse distance interpolations are only sensitive to the distance between the data and interpolation points, these basic schemes are really only adequate for truly discrete scattered data. In fluid dynamics and heat transfer calculations, the data is not truly discrete where the cell centre data, used in the interpolation, are come from averaging of distributed data inside the cell. Consider a vertex v located at the centre of a Voronoi-dual, as shown in Fig. 1. Laplacian of at the vertex can be derived from Gauss transformation of the φ in the Voronoi-dual.

$$\nabla^2\varphi = \frac{1}{\Omega}\int_S \nabla\varphi\cdot\vec{n}\; dS \tag{2}$$

Ω and S are the volume and surface area of the Voronoi-dual, respectively. n is a unit vector in the direction normal to the surface. In the case of the two-dimensional cell, Ω and S are the area and face length of the Voronoi-dual. If φ is considered to be linearly distributed inside the Voronoi-dual cell, $\nabla^2\varphi$ is equal to zero. While, $\nabla\varphi\cdot\vec{n}$ can be estimated as $(\varphi_i-\varphi_v)/l_i$ where φ_i and φ_v are φ a cell centre i and vertex v, respectively; l_i is an Euclidean distance between vertex v and cell centre i. Eq. (2) can then be rearranged for φ_v.

$$\varphi_v = \frac{\sum_{i=1}^{m}\frac{S_i}{l_i}\varphi_i}{\sum_{i=1}^{m}\frac{S_i}{l_i}} \tag{3}$$

In the two dimensional case, S_i is the face length of Voronoi-dual cell perpendicular to the line connecting vertex v and cell i. m represents the number of cell centre around vertex v. φ_v calculated using Eq. 3 is second order-accurate as it was derived with the assumption of zero Laplacian. It is possible to determine S_i using the coordinates of vertex v and the coordinates of cell centres surrounding the vertex. However, implementing this exact solution in a computer program is not efficient because it need to find a determinant matrix in most cases of severe randomised unstructured mesh is indeterminate. In this work, S_i was determined through a geometric approach. If the finite volume cell are isosceles triangles, as presented in Fig. 2, the face length of the finite volume cell i can be written as $L_i = \sqrt{4A_i}$, with A_i is area of i^{th} cell. The face length of the Voronoi-dual cell, S_i , can be found easily from triangles abc and dec as in Eq. 4.

$$S_i = 2/3\sqrt{A_i} \tag{4}$$

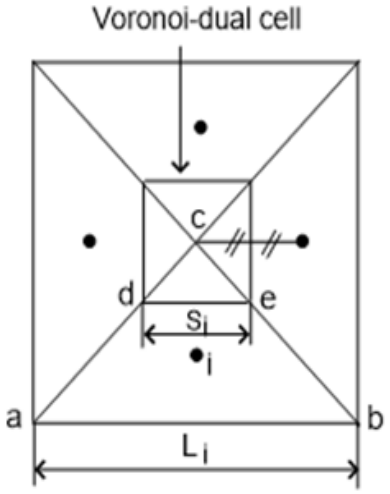

Figure 2: Isosceles-triangle cell

Substitute the S_i to Eq. (3), yield the equation for improved inverse distance interpolation.

$$\varphi_v = \frac{\sum_{i=1}^{n}\frac{A_i^{1/2}}{l_i}\varphi_i}{\sum_{i=1}^{n}\frac{A_i^{1/2}}{l_i}} \tag{5}$$

TEST CASE

Two two-dimensional potential flows were used as benchmarks. The first was a flow around an isolated cylinder in a uniform stream. The hydrodynamics solution of the flow is based on a doublet, the superimposed source and sink of equal strength, can be found in the textbook of White [19]. To investigate the effect of cell size on the accuracy, mesh refinement was made using three different numbers of cells; 1363, 11976 and 131898. The calculation domain and the mesh are shown in Fig. 3. The second hydrodynamics test case was a flow around a symmetrical Joukowsky aerofoil. This flow was derived from flow around a cylinder by a series of conformal transformations where lift on the cylinder was modelled by imposing circulation on the circle plane flow, the value being determined by the satisfaction of the Kutta condition in the aerofoil plane. Conformal mapping solutions for this type of flow may be found in the textbooks of Milne-Thomson [20], Vallentine [21] and Glauert [22]. Fig. 4 shows the calculation domain and mesh of the Joukowsky aerofoil. Following the procedure used by Syrakos [23] and Tasri [24], the accuracy test of the adjusted inverse distance weighted interpolations were carried out by interpolating the exact value of x-component of velocity from cell centres to cell vertices. The interpolated and exact values at the vertices were then used to calculate the L1 norm of errors.

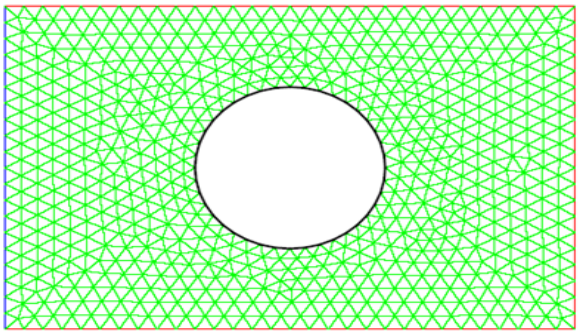

Figure 3: Calculation domain and mesh of flow pass circular cylinder

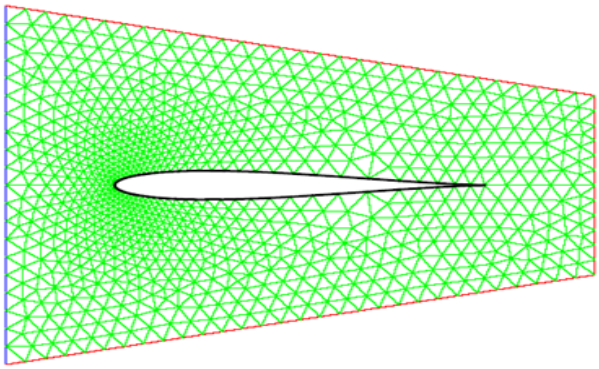

Figure 4: Calculation domain and mesh of flow pass Joukowsky aerofoil

The L1 norm error of interpolation of field variable φ from cell centres to vertices using standard and improved IDW interpolation for flow pass circular cylinder and Joukowsky aerofoil are shown in Fig. 5 and Fig. 6, respectively. In the flow pass circular cylinder, both interpolations have accuracy slightly higher than first order. Whereas, in the flow, through the Joukowsky aerofoil, the both interpolations, were only first-order accurate. This condition can be explained by writing φ at the cell centre i^{th} in term of the exact value of φ at vertex v using Taylor series expansion.

$$\varphi_i = \varphi'_v + \Delta x_i \frac{\partial \varphi}{\partial x} + \Delta y_i \frac{\partial \varphi}{\partial y} + \Delta z_i \frac{\partial \varphi}{\partial z} + O\left(\Delta^2\right) \tag{6}$$

where φ'_v is exact value of φ at vertex v. Substitute φ^i in Equation (5) with Equation (6) result

$$\varphi_v = \frac{\sum_{i=1}^{n}\left[\frac{A_i^{0.5}}{l_i}\left(\varphi'_v + \Delta x_i \frac{\partial \varphi}{\partial x} + \Delta y_i \frac{\partial \varphi}{\partial y} + \Delta z_i \frac{\partial \varphi}{\partial z} + O\left(\Delta^2\right)\right)\right]}{\sum_{i=1}^{n}\frac{A_i^{0.5}}{l_i}} \tag{7}$$

Reorder Equation (7) for the interpolation error, yield

$$\varphi_v - \varphi'_v = \frac{\frac{\partial \varphi}{\partial x}\sum_{i=1}^{n}\Delta x_i \frac{A_i^{0.5}}{l_i} + \frac{\partial \varphi}{\partial y}\sum_{i=1}^{n}\Delta y_i \frac{A_i^{0.5}}{l_i} + \frac{\partial \varphi}{\partial z}\sum_{i=1}^{n}\Delta z_i \frac{A_i^{0.5}}{l_i}}{\sum_{i=1}^{n}\frac{A_i^{0.5}}{l_i}} + O\left(\Delta^2\right) \tag{8}$$

The term $\varphi_v - \varphi'_v$ is the interpolation error. Eq. 8 shows that the interpolation will be second-order if the first term of the right-hand side vanishes. This condition holds if the conditions in Eq. 9 are satisfied

$$\sum_{i=1}^{n}\Delta x_i \frac{A_i^{0.5}}{l_i} = 0 \quad \sum_{i=1}^{n}\Delta y_i \frac{A_i^{0.5}}{l_i} = 0 \quad \sum_{i=1}^{n}\Delta z_i \frac{A_i^{0.5}}{l_i} = 0 \tag{9}$$

Eq. 9 can be satisfied if the cell centres are evenly distributed around the interpolation point. If these conditions are not met, the interpolation will only be accurate to first order. The figures also show that compared to standard IDW the adjusted inverse distance interpolation seems to be able to reduce errors significantly even though the degree of accuracy remains the same. The increase in interpolation accuracy is significant in finite volume solutions [25, 26]. A high interpolation accuracy provides better mass and momentum conservation at each iteration step so that the rate of convergence and accuracy is increased. Nevertheless, the cell area-weighted inverse distance is also valuable for accurately plotting the results of numerical calculations in the form of contour plots and XY plots.

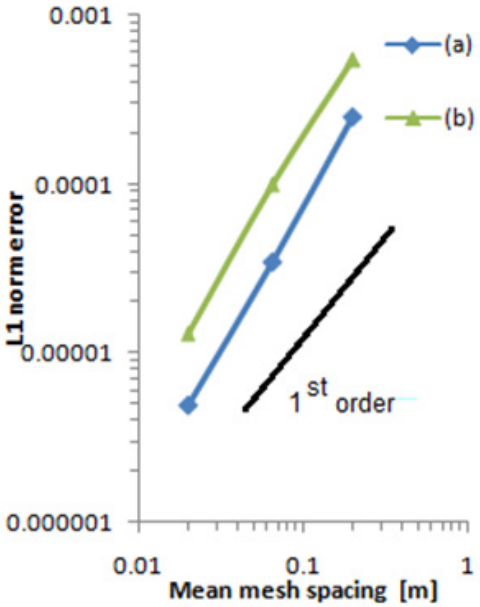

Figure 5: L1 error of Interpolation to vertices in flow pass circular cylinder. (a) Adjusted inverse distance interpolation (b) Standard inverse distance interpolation

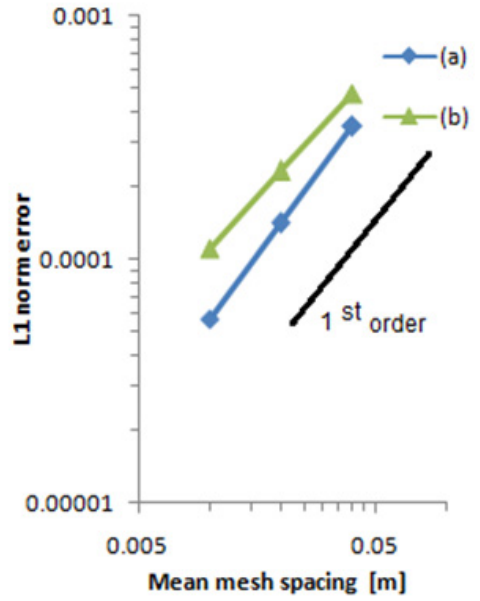

Figure 6: L1 error of Interpolation to vertices in the flow pass Joukowsky aerofoil. (a) Adjusted inverse distance interpolation (b) Standard inverse distance interpolation

CONCLUSION

A simple improvement to inverse distance interpolation was carried out in this work. It was found that:

1. The standard and adjusted inverse distance interpolations have the first-order accuracy on Delaunay unstructured finite volume meshes.
2. Compared to the standard inverse distance interpolation, the adjusted version of the interpolation has a lower L1 norm error.

REFERENCES

1. Tasri, A. (2021). Accuracy of cell centres to vertices interpolation for unstructured mesh finite volume solver, J. Inst. Eng. India Ser. C, vol. 102, 557-584. DOI: 10.1007/s40032-021-00697-5
2. Tasri, A. (2010). Simple improvement of momentum interpolation equation for Navier-Stoke equation solver on unstructured grid, Journal of Mathematics and Statistics, vol. 6, 265-270.
3. Shepard, D. (1968). A two-dimensional interpolation function for irregularly-spaced data. Proceedings of the 1968 23rd ACM national conference. p. 517-524.
4. Frink, N.T. (1992). Upwind scheme for solving the Euler equations on unstructured tetrahedral meshes. AIAA journal, vol.1, 70-7, DOI: 10.2514/3.10884
5. Fluent AN. (2018). Ansys fluent theory guide. ANSYS Inc., USA.
6. Shen, C.Y, Reed, H.L, Foley, T.A. (1993). Shepard's interpolation for solution-adaptive methods. Journal of Computational Physics, vol. 106, 52-61, DOI: 10.1006/jcph.1993.1090
7. Akima, H. (1978). A method of bivariate interpolation and smooth surface fitting for irregularly distributed data points. ACM Transactions on Mathematical Software (TOMS), vol. 4, 148-59, DOI: 10.1145/355780.355786
8. Lu, G.Y., Wong, D.W. (2008). An adaptive inverse-distance weighting spatial interpolation technique. Computers & Geosciences, vol. 1, 1044-55, DOI: 10.1016/j.cageo.2007.07.010
9. Azpurua, M.A., Dos Ramos, K. (2010). A comparison of spatial interpolation methods for estimation of average electromagnetic field magnitude. Progress In Electromagnetics Research M, vol 14, 135-45. DOI: 10.2528/PIERM10083103
10. Gotway, C.A., Ferguson, R.B., Hergert, G.W., Peterson, T.A. (1996). Comparison of kriging and inverse-distance methods for mapping soil parameters. Soil Science Society of America Journal, vol. 4, 1237-47. DOI: 10.2136/sssaj1996.03615995006000040040x
11. Hooyberghs, J., Mensink, C., Dumont, G., Fierens, F. (2000). Spatial interpolation of ambient ozone concentrations from sparse monitoring points in Belgium. Journal of Environmental Monitoring, vol. 8, 1129-35. DOI: 10.1039/b612607n
12. Golkhatmi, N.S., Sanaeinejad, S.H., Ghahraman, B., Pazhand, H.R. (2012). Extended modified inverse distance method for interpolation rainfall. International Journal of Engineering Inventions, vol. 1, 57-65.

13. Ke, W., Cheng, H.P., Yan, D., Lin. C. (2011). The Application of cluster analysis and inverse distance weighted interpolation to appraising the water quality of three forks lake. Procedia Enveromental Science, vol. 10, 2511-2517. DOI: 10.1016/j.proenv.2011.09.391.
14. Franke, R., Nielson, G. (1980). Smooth interpolation of large sets of scattered data. International Journal for Numerical Methods in Engineering. vol. 15, 1691-704. DOI: 10.1002/nme.1620151110
15. Ohtake, Y., Belyaev, A., Alexa, M., Turk, G., Seidel, H.P. (2005). Multi-level partition of unity implicits, Acm Transactions on Graphic, vol. 22, 463-470. DOI: 10.1145/882262.882293
16. Liu Z, Zhang Z, Zhou C, Ming W, Du Z. (2021). An adaptive inverse-distance weighting interpolation method considering spatial differentiation in 3D geological modeling. Geosciences. Vol. 11, 51-69. DOI: 10.3390/geosciences11020051.
17. Henderson N, Pena L. (2017). The inverse distance weighted interpolation applied to a particular form of the path tubes Method: Theory and computation for advection in incompressible flow. Applied Mathematics and Computation. Vol. 11, 114-135. DOI: 10.3390/geosciences11020051
18. Maleika W. (2020). Inverse distance weighting method optimization in the process of digital terrain model creation based on data collected from a multibeam echosounder. Applied Geomatics. vol. 4, 397-407. DOI: 10.1007/s12518-020-00307-6
19. White, F.M. Fluid mechanics (2015). Mc Graw-Hill, New York.
20. Milne-Thomson, L.M. (1996). Theoretical hydrodynamics. Courier Corporation.
21. Vallentine, H.R. (1969). Applied hydrodynamics, S.I. Edition. Butterworths.
22. Glauert, H. (1937). The Elements of aerofoil and airscrew theory. Cambridge University Press, UK.
23. Syrakos, A., Varchanis, S., Dimakopoulos, Y., Goulas, A., Tsamopoulos, J. (2017). A critical analysis of some popular methods for the discretisation of the gradient operator in finite volume methods. Physics of Fluids, vol. 29, 127103. DOI: 10.1063/1.4997682
24. Tasri, A., Susilawati, A. (2021). Accuracy of compact-stencil interpolation algorithms for unstructured mesh finite volume solver. Heliyon, vol. 7, e06875. DOI: 10.1016/j.heliyon.2021.e06875.
25. Tasri, A. (2021). Applying One-Dimensional TVD Scheme to Unstructured Mesh Finite Volume Solver. (2021). Journal of Mechanical Engineering Research and Developments, vol. 44, 400-407.
26. Nishikawa, H., (2021). The QUICK scheme is a third order finite volume scheme with point valued numerical solutions. International Journal for Numerical Methods in Fluids, vol. 93, 2311-2338.

Paper submitted: 23.09.2021.
Paper accepted: 02.12.2021.